Board Filter Design to Improve Jitter in Power Supply Remote Sensing Applications

By Xiaopeng Wang

I. INTRODUCTION

A board filter is a solution for improving switching jitter in situations where noises are picked up during remote sensing [1]. Using Vishay's SiC451 DC/DC buck converter as an example, this paper analyzes the characteristics of the board filter solution and presents a design trade-off between jitter improvement and output impedance.

II. NOISE IN REMOTE SENSING APPLICATIONS

From the viewpoint of noise and jitter analysis, voltage signals at two remote sensing pins include not only the load's terminal voltage V_O, but also external interference noise picked up via radiation or coupling in remote sensing applications. The noises are equivalent to common mode noise v_{CM} and differential mode noise V_{DM}, as illustrated in Fig. 1 for a Vishay SiC451 power delivery system for remote sensing. V_{CM} and V_{DM} noise may cause large switching jitter and output voltage ripple, and the impact varies by PWM control architecture [2]. In general, ripple-based control or peak current mode constant frequency control is more susceptible to noise than voltage mode constant frequency control.

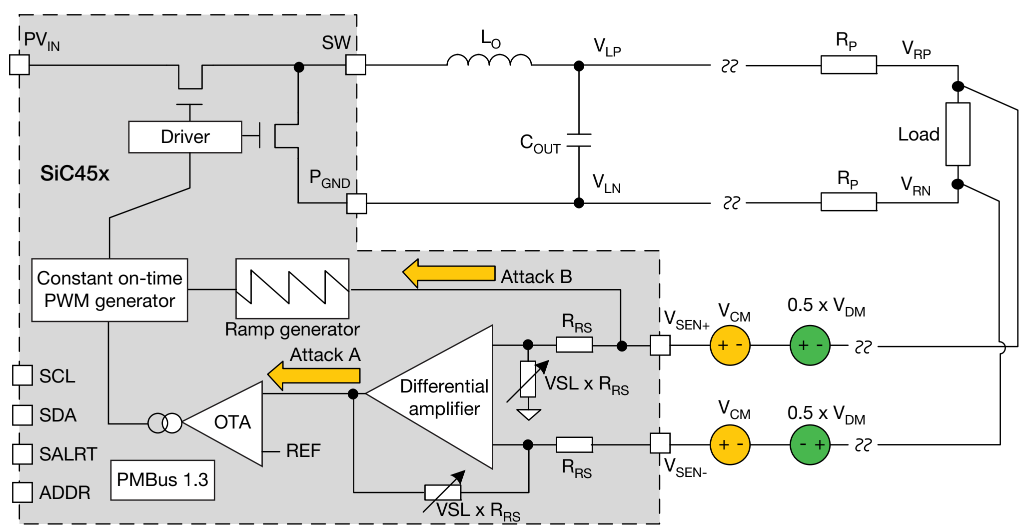

Fig. 1 - SiC451 and Noise Interference During Remote Sensing

The SiC451 in Fig. 1 is one device in a family of high efficiency microBUCK® DC/DC buck converters for PMBus 1.3 compatible and integrated ripple-based constant-on-time (COT) compensation with full differential remote sensing. Furthermore, four options for scaling down the VSL VOUT_SCALE_LOOP (VSL) factor are integrated so that the device can provide a wide 0.6 V to 12 V output voltage range without the need for voltage divider resistors. Therefore, the 5 mm x 7 mm SiC451 may only require a couple configuration resistors, making it an outstanding solution for high density power supplies in tight spaces.

Board Filter Design to Improve Jitter in Power Supply Remote Sensing Applications

As illustrated in Fig. 1, V_{CM} and V_{DM} may attack both the compensation circuit block and the ramp circuit block in the SiC451. The full differential sense amplifier across two remote sensing pins shall effectively reject V_{CM}, but may amplify V_{DM}. Meanwhile, both V_{CM} and V_{DM} may make the ramp signal noisy. Thus, if the noise is severe and not sufficiently constrained, cycle by cycle jitter and even large output voltage ripple contributed by low frequency sideband components [3] may be present in some applications. Fig. 2A presents an example of the SiC451 switching frequency jitter waveform in persistent mode when remote sensing pins are locally connected across the converter's output capacitor terminals. Fig. 2B presents the same signal when remote sensing pins are connected across the electronic load via a pair of 30 in. AWG30 wires. Due to the impact of noise picked up through the long remote sensing wires, the switching jitter was increased from 46.0 ns to 83.6 ns.

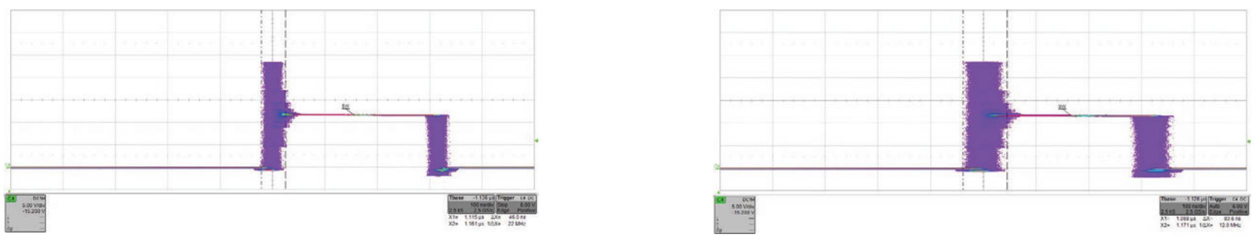

(A) local sensing

(B) remote sensing

Fig. 2 - Switching Frequency Jitter Increase From Remote Sensing Noise

III. BOARD FILTER SOLUTION

Having a passive filter onboard is one solution for reducing the amount of noise presented on the remote sensing pins. For example, it was reported that the solution successfully removed 33 kHz of oscillation from the output voltage, resulting in a low output ripple of 20 mV [4]. This paper analyzes the mechanism of the board filter solution and its design trade-off using the SiC451 DC/DC buck converter as an example.

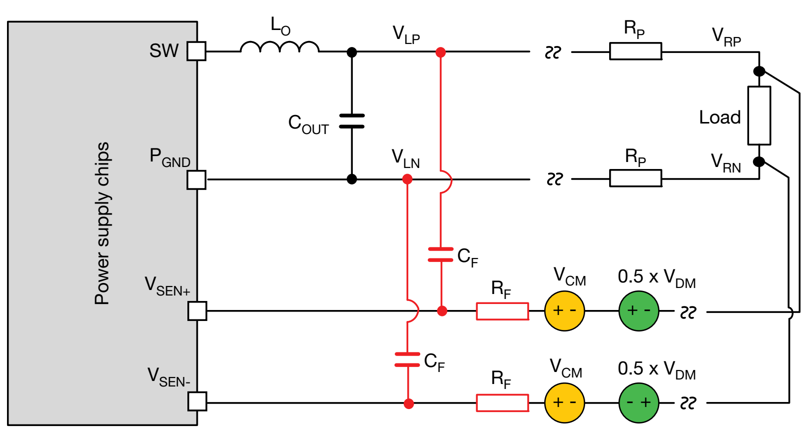

Fig. 3 - Board Filter Solution in Remote Sensing Applications

A complete board filter solution in remote sensing applications is illustrated in Fig. 3, where two pairs of discrete components, including two sensing resistors R_F and two bypass capacitors C_F, will be populated on the PCB board. V_{LP} and V_{LN} are voltages across the terminals of the converter's local output capacitors. V_{RP} and V_{RN} are voltages across the terminals of the converter's far distance loading chip. Power delivery rail impedance between the converter's local output capacitors and the loading chip is simplified to be resistance R_P.

The cutoff frequency f_F of the board filter solution is given in equation (1)

$$f_F = \frac{1}{2\pi \times R_F \times C_F} \qquad (1)$$

Board Filter Design to Improve Jitter in Power Supply Remote Sensing Applications

III. 1. LOOP DIAGRAM AND OPEN LOOP GAIN

A small signal loop diagram of a DC/DC buck converter without a board filter solution is depicted in Fig. 4A, and one with the board filter solution is depicted in Fig. 4B, where s is a complex number frequency parameter in the laplace transform. G_{VV} is the audio susceptibility transfer function from input voltage perturbation $\hat{V}_{IN}$ to output voltage $\hat{V}_O$; G_{VC} is the transfer function from regulator output perturbation $\hat{V}_C$ to $\hat{V}_O$; Z_O is the small signal open loop output impedance from load perturbation $\hat{I}_O$ to $\hat{V}_O$; T(s) is the open loop gain given in (2); K_{vDM} is the transfer function from remote sensing differential mode noise $\hat{V}_{DM}$ to output voltage $\hat{V}_O$; and K_{vCM} is the transfer function from remote sensing common mode noise $\hat{V}_{CM}$ to output voltage $\hat{V}_O$. Similarly, G_{SV}, G_{SC}, and Z_S are the audio susceptibility from $\hat{V}_{IN}$, the transfer function from $\hat{V}_C$, and the small signal open loop output impedance from $\hat{I}_O$ to the converter's remote sensing pin voltage $\hat{V}_S$; T_S (s) is the open loop gain of the converter with the board filter solution given in (3). A(s) is the remoting sensing noise's attenuation transfer function from the noise pickup location to the remote sensing pins, thanks to the board filter solution. G_C is the regulator transfer function from the signals $\hat{V}_O$ or $\hat{V}_S$ on the converter's V_{OUT} remote sensing pins to $\hat{V}_C$.

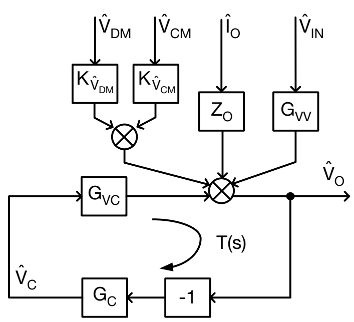

(A) No board filter solution

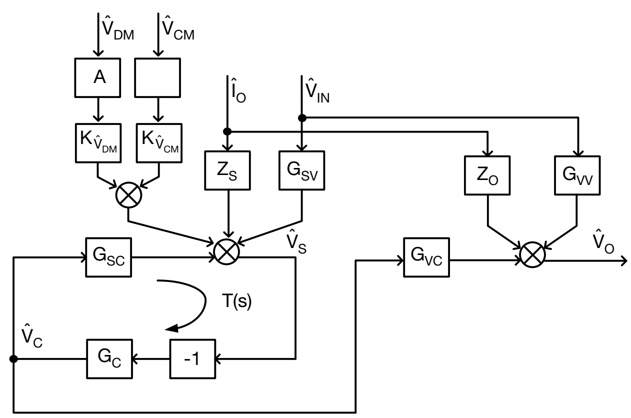

(B) With board filter solution

Fig. 4 - Small Signal Loop Diagram of DC/DC Converters

$$T(s) = G_C(s) \times G_{VC}(s) \tag{2}$$

$$T_S(s) = G_C(s) \times G_{SC}(s) \tag{3}$$

The power delivery path in Fig. 3 is redrawn in Fig. 5, where R_{load} is the small signal input impedance of the loading chip. Thus, $G_{SC}(s)$ can be derived from $G_{VC}(s)$ in (4), and $G_{SV}(s)$ can be derived from $G_{VV}(s)$ in (5).

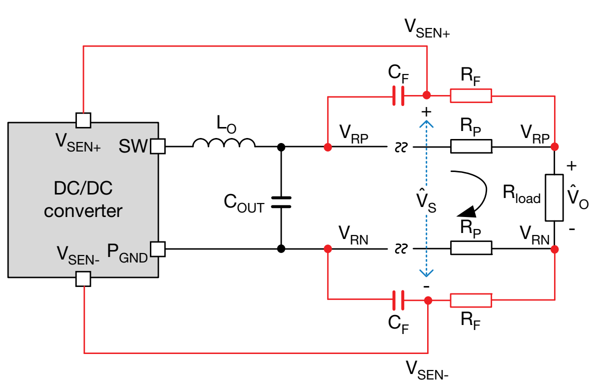

Fig. 5 - Power Delivery Path of DC/DC Buck Converter

Board Filter Design to Improve Jitter in Power Supply Remote Sensing Applications

$$G_{SC}(s) = G_{VC}(s) \times \frac{1 + (R_F + R_P) \times C_F \times s}{1 + \left(R_F + \frac{1}{1 + \frac{2 \times R_P}{R_{load}}} \times R_P\right) \times C_F \times s} \times \frac{1 + \left(1 + \frac{2 \times R_P}{R_{load}}\right) \times R_F \times C_F \times s}{1 + R_F \times C_F \times s} \quad (4)$$

$$G_{SV}(s) = G_{VV}(s) \times \frac{1 + (R_F + R_P) \times C_F \times s}{1 + \left(R_F + \frac{1}{1 + \frac{2 \times R_P}{R_{load}}} \times R_P\right) \times C_F \times s} \times \frac{1 + \left(1 + \frac{2 \times R_P}{R_{load}}\right) \times R_F \times C_F \times s}{1 + R_F \times C_F \times s} \quad (5)$$

$$2 \times R_P \ll R_{load} \quad (6)$$

According to (4) and (5), when the criteria of $2 \times R_P \ll R_{load}$ in (6) is satisfied - which means that the power delivery rail resistance R_P is much less than R_{load} in normal practice – the differences between G_{VC} and G_{SC} and between G_{VV} and G_{SV} are both ignorable, as is the difference between T(s) and T_S(s) based on (2) and (3).

For those cases where R_P is not smaller than R_{load}, the difference between G_{VC} and G_{SC} and the difference between G_{VV} and G_{SV} shall also be ignorable below the cutoff frequency f_F of the board filter. At the same time, for those frequencies above the cutoff frequency f_F, G_{SC} and G will still be at maximum a factor of $(1 + (2 \times R_P)/R_{load})$ larger than G_{VC} and G_{VV}, provided that $R_P \ll R_F$.

An example SiC451 buck converter is used to verify the loop dynamics difference before and after adding the board filter solution. The example system's configuration parameters are listed in Table 1.

TABLE 1 - CONFIGURATION PARAMETERS OF THE EXAMPLE SiC451 SYSTEM

SYMBOL	DESCRIPTION	VALUE		SYMBOL	DESCRIPTION	VALUE
V_{IN} (V)	Input voltage	12		R_P (mΩ)	Power rail resistance	1.7
V_{OUT} (V)	Output voltage	3.3		R_F (Ω)	Filter resistance	51
F_{SW} (kHz)	Switching frequency	800		C_F (µF)	Filter capacitance	1
L (nH)	Power inductance	0.47		DCR (mΩ)	DCR of power inductor (1)	1
C_{OUT} (µF)	Output capacitance	400		R_{EQU} (mΩ)	Equivalent resistance in power stage (1)	3
I_{OUT} (A)	DC output current	15		R_{ESR} (mΩ)	ESR of output capacitors (1)	1

Note

(1) The values used in Simplis simulation

The simulation data of T(s) and T_S(s) in a Simplis environment, including crossover frequency, gain margin, and phase margin, are listed in Table 2, where four scenarios of R_{load} and two values of R_F (0.2 Ω and 51 Ω) corresponding to a much different f_F are tested. The data in Table 2 align with the above analysis and demonstrate that the open loop gain difference between T(s) and T_S(s) is ignorable as expected when $R_P \ll R_{load}$. And the difference will be further decreased when cutoff frequency f_F of the board filter moves higher.

Board Filter Design to Improve Jitter in Power Supply Remote Sensing Applications

TABLE 2 - OPEN LOOP GAIN SIMULATION DATA							
SCENARIOS	T(s)			T_S(s)			
$\frac{R_{load}}{R_P}$	CROSSOVER FREQUENCY (kHz)	PHASE MARGIN (°)	GAIN MARGIN (dB)	f_F (kHz)	CROSSOVER FREQUENCY (kHz)	PHASE MARGIN (°)	GAIN MARGIN (dB)
∞ (constant current load, 15 A)	94.75	75.52	19.25	796	94.75	75.52	19.25
				3.12	94.75	75.52	19.25
500 (resistive load)	94.31	75.7	19.27	796	94.32	75.72	19.27
				3.12	94.69	75.69	19.25
100 (resistive load)	92.43	77.05	19.65	796	92.46	77.16	19.66
				3.12	94.22	76.99	19.5
20 (resistive load)	83.69	83.18	21.34	796	83.79	83.65	21.33
				3.12	92	82.51	20.52

Note
- R_P = 1.7 mΩ, C_F = 1 μF

III. 2. OUTPUT IMPEDANCE

The open loop output impedance $Z_O(s)$ in Fig. 4A is given in (7), where $Z_{LC}(s)$ is the open loop output impedance of the power stage and is given in (8). L is the inductance of the power inductor; R_{EQU} is the equivalent resistance in the power stage, including the inductor's DC resistance (DCR) and duty cycle weighted power FET on resistance $R_{DS(on)}$; C_{OUT} and R_{ESR} is the output capacitors' capacitance and equivalent series resistance (ESR).

$$Z_O(s) = 2 \times R_P + Z_{LC}(s) \tag{7}$$

$$Z_{LC}(s) = \frac{(L_S + R_{EQU}) \times ((R_{ESR} \times C_{OUT} \times s) + 1)}{LC_{OUT} \times s^2 + ((R_{EQU} + R_{ESR}) \times C_{OUT} \times s) + 1} \tag{8}$$

Furthermore, $Z_S(s)$ in Fig. 4B is given in (9) under the assumption that the criteria (6) is satisfied.

$$Z_S(s) = Z_O(s) \times \left[1 - \frac{2 \times R_P}{2 \times R_P + Z_{LC}(s)} \times \frac{R_F \times C_F \times s}{(R_F \times C_F \times s) + 1}\right] \tag{9}$$

The closed loop output impedance $Z_{O\_S}^{closed}(s)$ with a board filter solution is given in (10), where $Z_O^{closed}(s)$ derived in (11) is the closed loop output impedance without a board filter solution.

$$Z_{O\_S}^{closed}(s) = Z_O(s) - Z_S(s)\frac{G_C(s) \times G_{VC}(s)}{1 + T_S(s)} \tag{10}$$

$$Z_{O\_S}^{closed}(s) = \frac{Z_O(s)}{1 + T_S(s)} \tag{11}$$

After introducing (7) and (9) into (10), and ignoring the difference between T(s) and $T_S(s)$, the relation between $Z_{O\_S}^{closed}(s)$ and $Z_o^{closed}(s)$ is concluded in (12).

$$Z_{O\_S}^{closed}(s) = Z_O^{closed}(s) + Z_o(s)\frac{T(s)}{1 + T(s)} \times \frac{2 \times R_P}{2 \times R_P + Z_{LC}(s)} \times \frac{R_F \times C_F \times s}{(R_F \times C_F \times s) + 1} \tag{12}$$

$Z_{O\_S}^{closed}(s)$ in (12) is the sum of $Z_O^{closed}(s)$ and an additional term determined by R_P, f_F, $Z_{LC}(s)$, and T(s), which indicates that the board filter may increase the closed loop output impedance of the power converter while it improves noise susceptibility.

Board Filter Design to Improve Jitter in Power Supply Remote Sensing Applications

For the converters without applying remote sensing, the closed loop output impedance $Z_{O\_L}^{closed}(s)$ is given in (13). As the power rail resistance R_P is not included in the controller compensation loop, $Z_{O\_L}^{closed}(s)$ will be significantly larger than $Z_O^{closed}(s)$ and $Z_{O\_S}^{closed}(s)$ in the low frequency range.

$$Z_{O\_L}^{closed}(s) = \frac{Z_{LC}(s)}{1 + T(s)} + 2 \times R_P \tag{13}$$

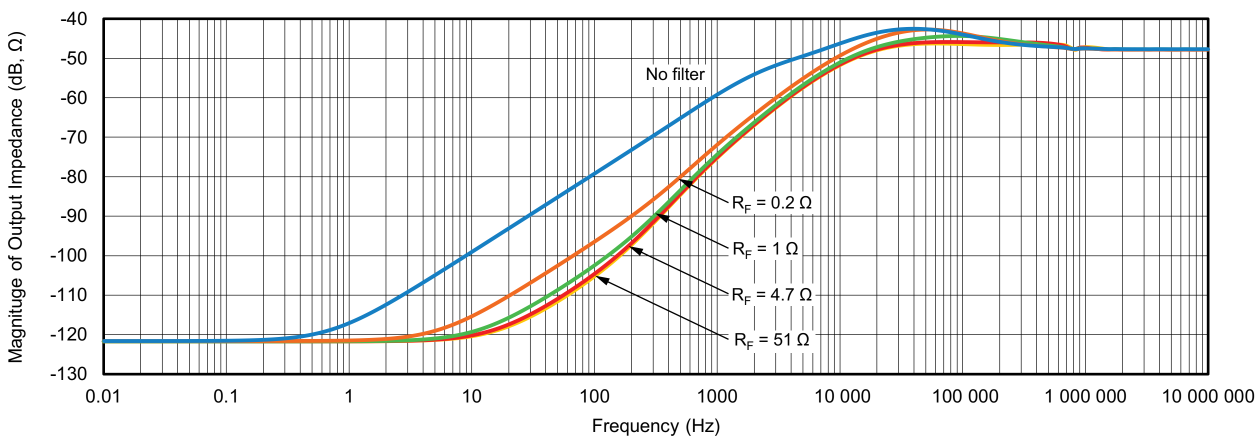

Fig. 6 - Magnitude of $Z_{O\_S}^{closed}(s)$

Fig. 6 illustrates $Z_{O\_S}^{closed}(s)$ of the example SiC451 specified in Table 1, where four different R_F - 0.2 Ω, 1 Ω, 4.7 Ω, and 51 Ω, respectively - and a 15 A constant current load were used in a Simplis simulation. Furthermore, the simulation data of the closed loop output impedance in several frequencies are listed in Table 3 and were compared with their analytical values calculated from (11), (12), and (13). Table 3 verified that the analytical values of the three kinds of closed-loop output impedance match the simulation data in a Simplis environment.

TABLE 3 - MAGNITUDE OF THE CLOSED LOOP OUTPUT IMPEDANCE

SCENARIOS			FREQUENCY (kHz)						
			0.3	1	10	69	120	398	832
$\lvert Z_{O\_L}^{closed}(s)\rvert$ (mΩ)	No remote sensing; no filter	Simulation	3.39	3.32	4.88	7.43	6.33	4.84	4.43
		Equation	3.41	3.5	5.96	7.49	6.54	5	4.49
$\lvert Z_O^{closed}(s)\rvert$ (mΩ)	Remote sense; no filter	Simulation	0.027	0.18	2.78	5.26	5.13	5.13	4.37
		Equation	0.024	0.17	2.59	5.04	4.99	5.11	4.34
$\lvert Z_{O\_S}^{closed}(s)\rvert$ (mΩ)	f_F = 796 kHz	Simulation	0.028	0.19	2.81	5.48	5.45	5.39	4.46
		Equation	0.025	0.17	2.63	5.28	5.34	5.4	4.46
	f_F = 159 kHz	Simulation	0.032	0.2	2.97	6.42	6.43	5.16	4.44
		Equation	0.03	0.18	2.79	6.3	6.41	5.19	4.45
	f_F = 33.9 kHz	Simulation	0.054	0.27	3.69	7.73	6.67	4.91	4.43
		Equation	0.052	0.25	3.53	7.73	6.69	4.92	4.43
	f_F = 3.12 kHz	Simulation	0.348	1.16	5.22	7.5	6.37	4.84	4.42
		Equation	0.346	1.15	5.17	7.5	6.37	4.85	4.42

Note

- R_P = 1.7 mΩ, C_F = 1 µF

Board Filter Design to Improve Jitter in Power Supply Remote Sensing Applications

III. 3. AUDIO SUSCEPTIBILITY

Similar to the output impedance analysis, the closed loop audio susceptibility $G_{VV\_S}^{closed}(s)$ with the board filter solution is given in (14), where $G_{VV}^{closed}(s)$ derived in (15) is the closed loop input impedance without the board filter solution.

$$G_{VV\_S}^{closed}(s) = G_{VV}(s) - G_{SV}(s) \times \frac{G_C(s) \times G_{VD}(s)}{1 + T_S(s)} \tag{14}$$

$$G_{VV}^{closed}(s) = \frac{G_{VV}(s)}{1 + T(s)} \tag{15}$$

After ignoring the difference between T(s) and $T_S(s)$ and the difference between $G_{VV}(s)$ and $G_{SV}(s)$, the relation between $G_{VV\_S}^{closed}(s)$ and $G_{VV}^{closed}(s)$ is derived in (16), which indicates that the board filter solution has an ignorable impact on the audio susceptibility.

$$G_{VV\_S}^{closed}(s) = G_{VV}^{closed}(s) \tag{16}$$

Fig. 7 illustrates the closed loop audio susceptibility of the example SiC451 specified in Table 1, where C_F = 1 µF, four different R_F were chosen as 0.2 Ω, 1 Ω, 4.7 Ω, and 51 Ω, respectively, and a 15 A constant current load is used in a Simplis simulation. Fig. 7 verified the analysis that the board filter solution has an ignorable impact on the audio susceptibility.

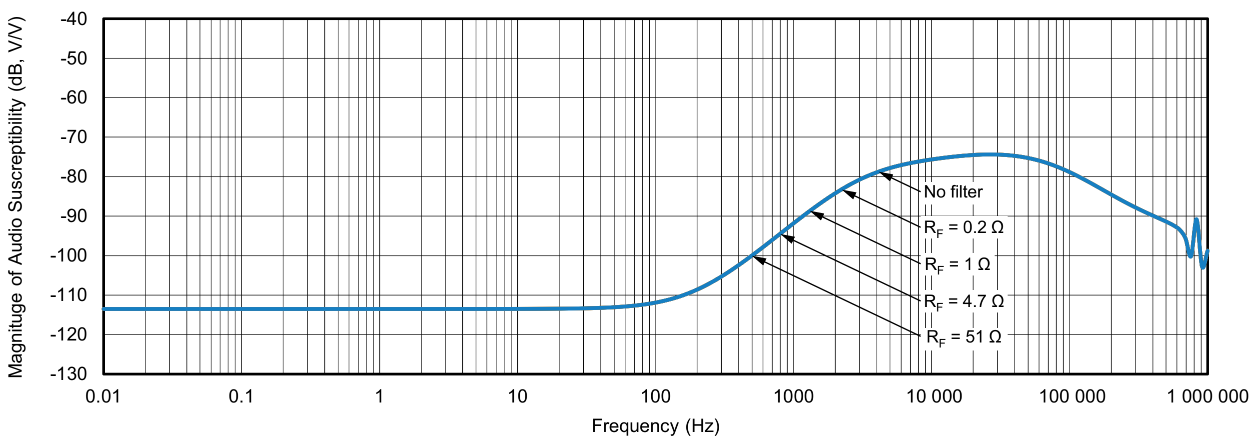

Fig. 7 - Magnitude of the Closed Loop Audio Susceptibility

III. 4. NOISE SUSCEPTIBILITY

For the sake of noise susceptibility analysis, the board filter solution in Fig. 3 is redrawn in Fig. 8 under an assumption that the input impedance of the power converter's remote sensing pin is infinite. The noise signal applied across node V_{SEN+} and node V_{RP} is analyzed under the superposition principle as the sum of two signals V^{N1} and V^{N2} generated by the noise V_{CM} and V_{DM}, respectively, on two differential remote sensing wires. The equation of V^{N1} is derived in (17) and that of V^{N2} is derived in (18) after simplification based on the criteria (6) and an assumption of $R_P \ll R_F$.

Board Filter Design to Improve Jitter in Power Supply Remote Sensing Applications

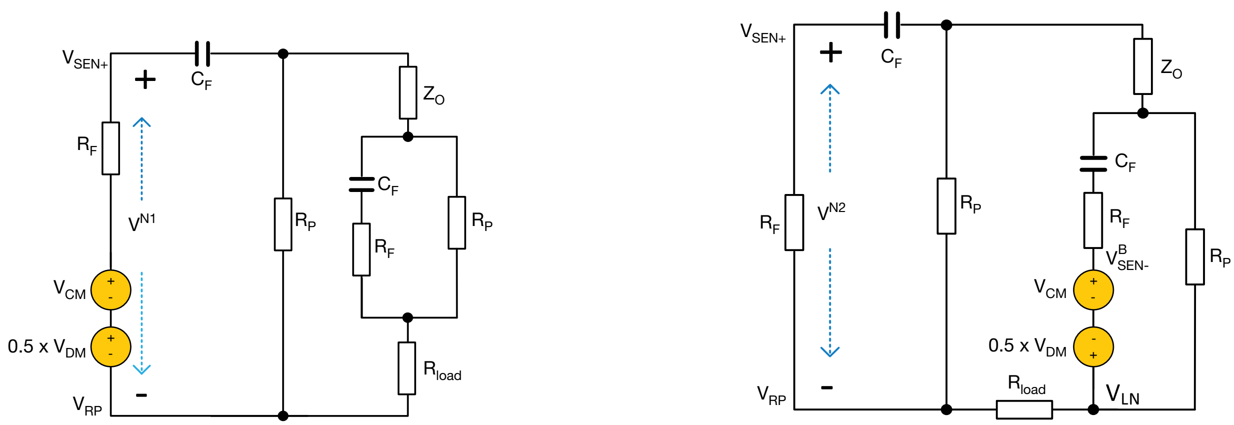

(A) VN1 from noise on the VSEN+ sense line (B) VN2 from noise on the VSEN- sense line

Fig. 8 - Superposition Analysis of Noises on V_{SEN+} Pin

$$V^{N1} = \frac{1 + R_P \times C_F \times s}{1 + R_F \times C_F \times s} \times (V_{CM} + 0.5 \times V_{DM}) \tag{17}$$

$$V^{N2} = \frac{R_P \times C_F \times s}{1 + R_F \times C_F \times s} \times \frac{R_P}{R_P + Z_{LC} + R_{load}} \times \frac{R_F \times C_F \times s}{1 + R_F \times C_F \times s} \times (V_{CM} - 0.5 \times V_{DM}) \tag{18}$$

It can be concluded from (17) and (18), when criteria (6) $2 \times R_P \ll R_{load}$ exists, V^{N2} will be much less than V^{N1} in magnitude and V^{N1} will dominate the noise across node V_{SEN+} and node V_{RP}. The same conclusion can be applied to the noise attenuation across node V_{SEN-} and node V_{RN}. Thus, an approximate expression of the remote sensing noise's attenuation function A(s) can be derived in (19).

$$A(s) = \frac{1 + R_P \times C_F \times s}{1 + R_F \times C_F \times s} \tag{19}$$

The magnitude of the attenuation function A(s) in the example SiC451 application specified in Table 1 is depicted in Fig. 9, where C_F = 1 μF, and four different R_F were chosen as 0.2 Ω, 1 Ω, 4.7 Ω, and 51 Ω, respectively. The magnitude of the attenuation function in several frequencies is listed in Table 4.

Board Filter Design to Improve Jitter in Power Supply Remote Sensing Applications

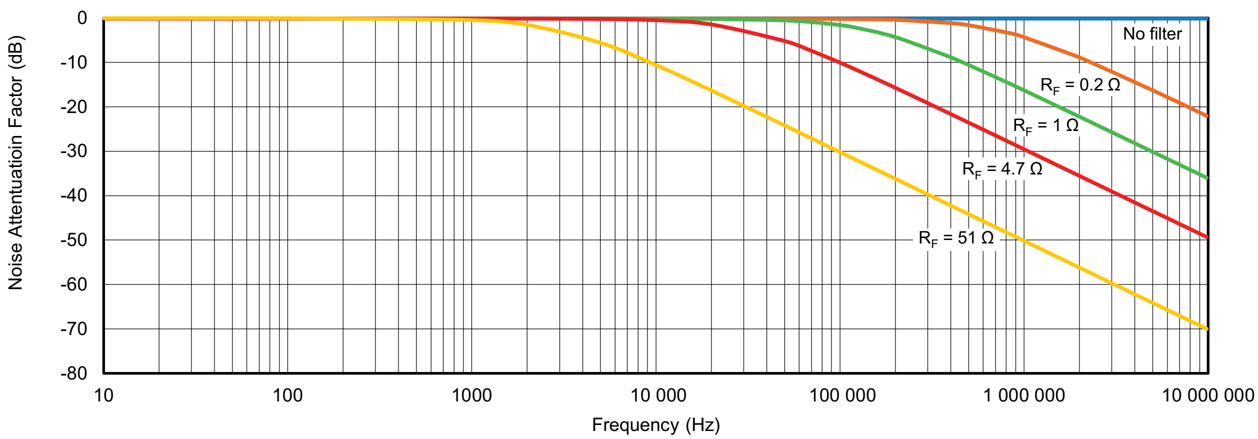

Fig. 9 - Noise Attenuation of the Board Filter Solution

TABLE 4 - MAGNITUDE OF THE NOISE ATTENUATION FUNCTION

SCENARIOS		FREQUENCY (kHz)						
		1	10	69	120	398	832	2089
|A(s)| (dB, V/V)	No filter	0	0	0	0	0	0	0
	f_F = 796 kHz	0	0	-0.03	-0.10	-0.97	-3.21	-8.97
	f_F = 159 kHz	0	-0.02	-0.75	-1.96	-8.61	-14.52	-22.39
	f_F = 33.9 kHz	0	-0.36	-7.14	-11.34	-21.44	-27.81	-35.80
	f_F = 3.12 kHz	-0.42	-10.52	-26.92	-31.72	-42.12	-48.51	-56.51

Note

- R_P = 1.7 mΩ, C_F = 1 μF

III. 5. FILTER DESIGN

The analysis in section III. 2. and III. 4. indicates a trade-off between the output impedance and noise attenuation in the design of the board filter. Besides the above linear analysis, for converters like the SiC451, typical of ripple-based control, the capacitor C_F in the board filter will bypass high frequency V_{OUT} ripple across the converter's local output capacitors and the resistor R_F will attenuate a distorted V_{OUT} ripple remotely sensed at a far distance loading site. Therefore, the board filter will improve the fidelity of V_{OUT} ripple and keep the performance of the controller from the influence of the power delivery path's electrical characteristic.

Board Filter Design to Improve Jitter in Power Supply Remote Sensing Applications

A. Cutoff Frequency f_F

As illustrated in (12) and (19), the cutoff frequency f_F of the filter determines the trade-off between the output impedance and noise attenuation. When the cutoff frequency f_F is chosen higher, the second term in (12) will be less for those frequencies below the controller's open loop gain crossover frequency. Meanwhile, the magnitude of attenuation function in (19) will be decreased at the same time.

The choice of the cutoff frequency f_F depends on noise characteristics and jitter requirements in specific applications. Because the open loop gain crossover frequency in the example SiC451 system is designed to one eighth of the switching frequency, the cutoff frequency is set to be one third of the crossover frequency, so that a 28 dB noise attenuation is achieved around the switching frequency.

B. Resistance R_F

For a determined cutoff frequency f_F, a large filter resistance R_F will minimize the profile of the capacitor C_F and decrease the difference between (4) and (5). On the other hand, however, a large filter resistance R_F may degrade V_{OUT} accuracy when the input impedance of the power converter's sensing amplifier is not infinite.

For the example SiC451 system, R_F is selected to be 4.7 Ω and C_F is selected to be 1.0 μF.

III. 6. EXPERIMENT DATA

Jitter, ripple, and load transients of the example SiC451 system were tested in three scenarios clarified in Table 5 based on whether either the remote sensing or board filter solution is applied. The definition of the three scenarios is clarified in Table 5. The switching frequency jitter waveforms in the three scenarios were given in Fig. 10; the ripple in the three scenarios were given in Fig. 11; the loading transients were given in Fig. 12, where the load current rose from 5 A to 15 A in 50 μs. Switching frequency jitter and V_{OUT} undershoot values during loading transients were summarized in Table 5.

TABLE 5 - EXPERIMENTAL SCENARIO AND DATA

	#1 SCENARIOS	#2 SCENARIOS	#3 SCENARIOS
Sensing point connection	Local output capacitors	Electronic load	Electronic load
Sensing wire parameters	3 in, 6 mil PCB trace	30 in AWG30 wires	30 in AWG30 wires
Board filter	None	None	R_F = 4.7 Ω, C_F = 1 μF
Switching frequency jitter at 15 A DC load	46.0 ns	83.6 ns	48.4 ns
V_{OUT} undershoot at 5 A to 15 A in 50 μs	101.5 mV	63.5 mV	65.0 mV

Board Filter Design to Improve Jitter in Power Supply Remote Sensing Applications

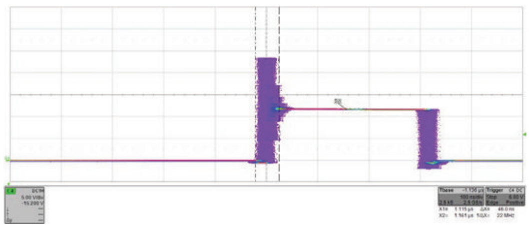

(A) No remote sensing

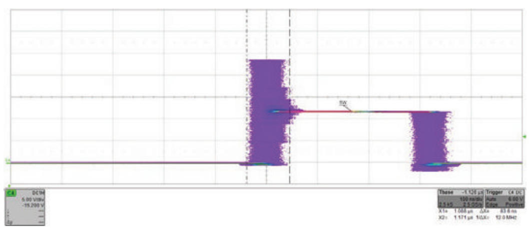

(B) No board filter

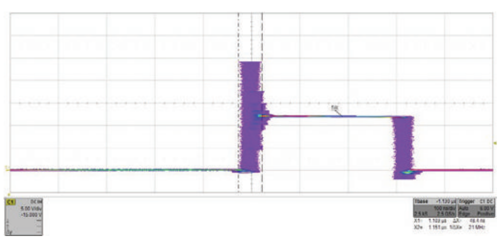

(C) With board filter

Fig. 10 - Switching Frequency Jitter With 15 A_{DC} Load

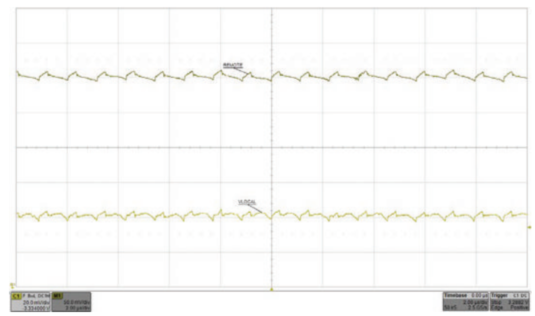

(A) No remote sensing

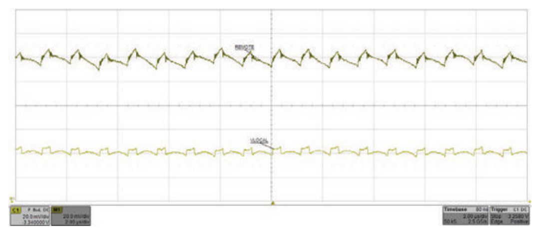

(B) No board filter

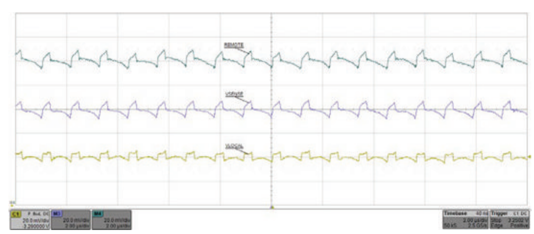

(C) With board filter

Fig. 11 - V_{OUT} Ripple With 15 A_{DC} Load

A. Switching Jitter

Fig. 10(B) shows that the remote sensing noise increased the switching jitter by 82 %.

Fig. 10(C) shows that the jitter was effectively mitigated after applying the board filter solution and the jitter increase is minimized to only 5 %.

Board Filter Design to Improve Jitter in Power Supply Remote Sensing Applications

B. Loading Transient

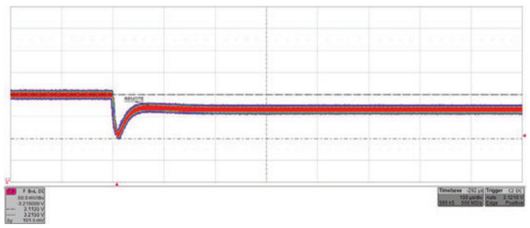

(A) No remote sensing

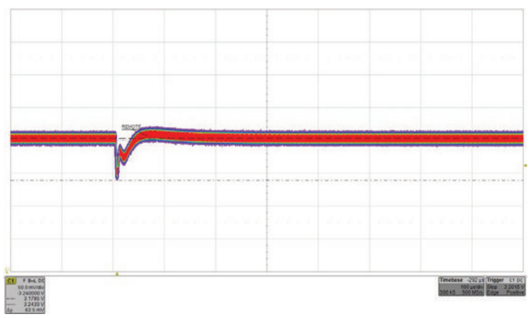

(B) No board filter

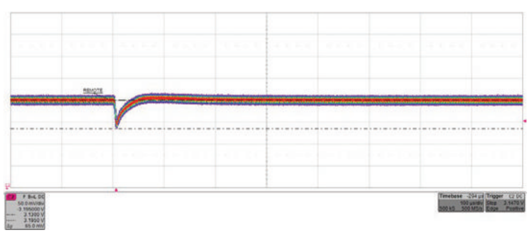

(C) With board filter

Fig. 12 - Loading Transient

V_{OUT} undershoot in Fig. 12(B) and Fig. 12(C) verified the advantage of remote sensing in consideration of loading transients, in which V_{OUT} undershoot was improved by 37 % and 36 % from the one in Fig. 12(A) without remote sensing.

V_{OUT} undershoot in Fig. 12(C) with the board filter solution is almost the same as the one in Fig. 12(B) without the board filter solution. This explains why the output impedance analysis in section III. 2. did not take the impact of remote sensing noise into account, and that the latter may increase closed-loop output impedance to some extent for the system without the board filter solution in real applications. The remote sensing noise may deteriorate the V_{OUT} undershoot in two ways. First, the noise will generate low frequency sideband components in V_{OUT} and make V_{OUT}ripple larger, which is observable in Fig. 11 (B) and Fig. 12 (B). Second, as SiC451 is a ripple-based constant on-time converter, the board filter will improve fidelity of V_{OUT} ripple on the remote sensing pins and keep performance of the controller from the influence of the power delivery path. Fig. 12 (C) presented a similar V_{OUT} dynamic response to Fig. 12 (A), while Fig. 12 (B) presented a different one.

IV. CONCLUSION

Remote sensing is a popular measure for improving the output voltage quality of power converters, but the noise pickup on the remote sensing wires may cause large switching jitter and V_{OUT} ripple. This paper developed equations to explain the different effects on loop gain, output impedance, audio susceptibility, and noise attenuation when a board filter solution is utilized to mitigate the remote sensing noises. Using Vishay's SiC451 DC/DC buck converter as an example, the paper presents simulation data of those features when several kinds of filter cutoff frequency were applied to demonstrate the design tradeoff between jitter improvement and output impedance. Experimental data verified considerations in the paper and demonstrated the efficiency of the board filter solution on mitigating remote sensing noise to improve switching jitter.

REFERENCES

[1] Kris Dehnel, Amanda Alfonso, "Solving the Technical Challenges of Powering High-Density Logic Devices", Intel white paper

[2] Matt Schurmann, "Not All Jitter is Created Equal: Understanding Jitter in Switching power Supplies", Texas Instruments Application report, SLUA747A, July 2015

[3] Yang Qiu, Ming Xu, Juanjuan Sun, Fred C. Lee, "A generic high-frequency model for the nonlinearities in Buck converters," IEEE Transactions on Power Electronics, Vol. 22, Issue: 5, Sept. 2007

[4] Tiger Zhou, "Remote Sensing for Power Supplies," Texas Instruments Application Note, SLYT467, 2012